

## **LOCAL SCOUR AROUND SPUR DIKES**

**M. M. Ezzeldin<sup>1</sup>, T. A. Saafan<sup>2</sup>, O. S. Rageh<sup>3</sup> and L. M. Nejm<sup>4</sup>**

<sup>1,2</sup> Professors, <sup>3</sup> Associate Professor, <sup>4</sup> Teaching Assistant  
Irrigation and Hydraulics Department, Faculty of Engineering,  
Mansoura University, El-Mansoura, Egypt

### **ABSTRACT**

A series of experiments were conducted to study the phenomenon of local scour that takes place beside a single spur dike installed as a training structure on straight channel, and to investigate the relation between the dimensions of the scour hole and between non-dimensional parameters describing the flow ratio, and angle of flow attack. All tests were held under clear-water condition, using a horizontal bed consisted of non-uniform sandy soil ( $D_{50}= 0.6\text{mm}$ ). Several equations were obtained to compute the relative maximum scour hole depth and length. Results showed that the computed scour depths were in agreement with the experimental scour depths.

### **INTRODUCTION**

A spur dike can be defined as an elongated structure having one end on the bank of a stream and the other end projecting into the current (Kuhnle et al., 1999). Spur dikes have been widely used to redirect the flow in channels and to protect eroding stream banks. They have also been used to enhance aquatic habitats by causing stable pools in unstable, disturbed streams.

Like any hydraulic structure, when a spur dike crosses a water way the natural balance of the river is disturbed, results in a major disturbance of the flow pattern around the structure base. This disturbance leads to the initiation of scour process. This scour is considered to be the major cause of structure foundations failure. Therefore, the problem of scour around any obstruction placed in an alluvial channel is of great importance to hydraulic engineers, because an accurate estimation of local scour beside these structures is very important for safe and economic design of their foundations.

There are many factors affect the scouring process. Researchers tried to study these factors separately, or made a combination between two or more factors. Garde stated that when all other variables held constant, the maximum scour depth had the greatest value for a spur dike inclination of  $90^\circ$ . For all other inclinations upstream or downstream, the scour depth was smaller. Tison (1962) disagreed with Garde's idea and he proved his point of view by conducting experiments using three angles namely  $72^\circ 30'$ ,  $90^\circ$  and  $107^\circ 30'$  and held all other variables constant. He found that the greatest maximum scour depth was recorded for the upstream spur-dike inclination. Melville found that the scour depth increase with an increase in  $\theta$ . Raudikivi agreed

with his idea and stated that the scour depth was reduced for  $\theta < 90^\circ$  and increased for  $\theta > 90^\circ$ . However the data by Kwan (1984) and Kandasany (1985), as cited in Raudikivi (1998), showed that the increase was only in the early stages of clear-water scour development (duration of experiments less than 5 hours), but the equilibrium scour depth was reduced for both  $\theta$  smaller and larger than  $90^\circ$ .

Zaghloul (1983) held an experimental work and found that the maximum depth is significantly affected by the channel's Froude number and the opening ratio at the spur-dike's location. Another experimental study were carried out by Kondap and Prayag (1989) in a flume on rigid and sand bed to determine the minimum length of spur by observing percentage increase in unit discharge defined as product of velocity and depth and scour depth near the nose of spur. The experimental works carried out on rigid bed with single spur has shown that  $b/B$  ratio of 0.2 is desirable as it causes minimum increase in the discharge intensity at the nose. Studies on the mobile bed with single spur have shown that beyond  $b/B$  ratio of 0.2, the scour near the nose increase rapidly. Further the scour near the nose is comparable to  $b/B$  ratio less 0.2 should be adopted in the design of spur for straight reach of a river.

This study aims to investigate the local scour phenomenon and the relation between the dimensions of the scour hole that takes place beside a single spur dike installed as a training structure on straight channel, and between flow parameters, contraction ratio and angle of inclination of the structure it self to the flow direction. Regression analysis was used to perform some formulas between the relative maximum scour depth and length against other parameters involved in the phenomena.

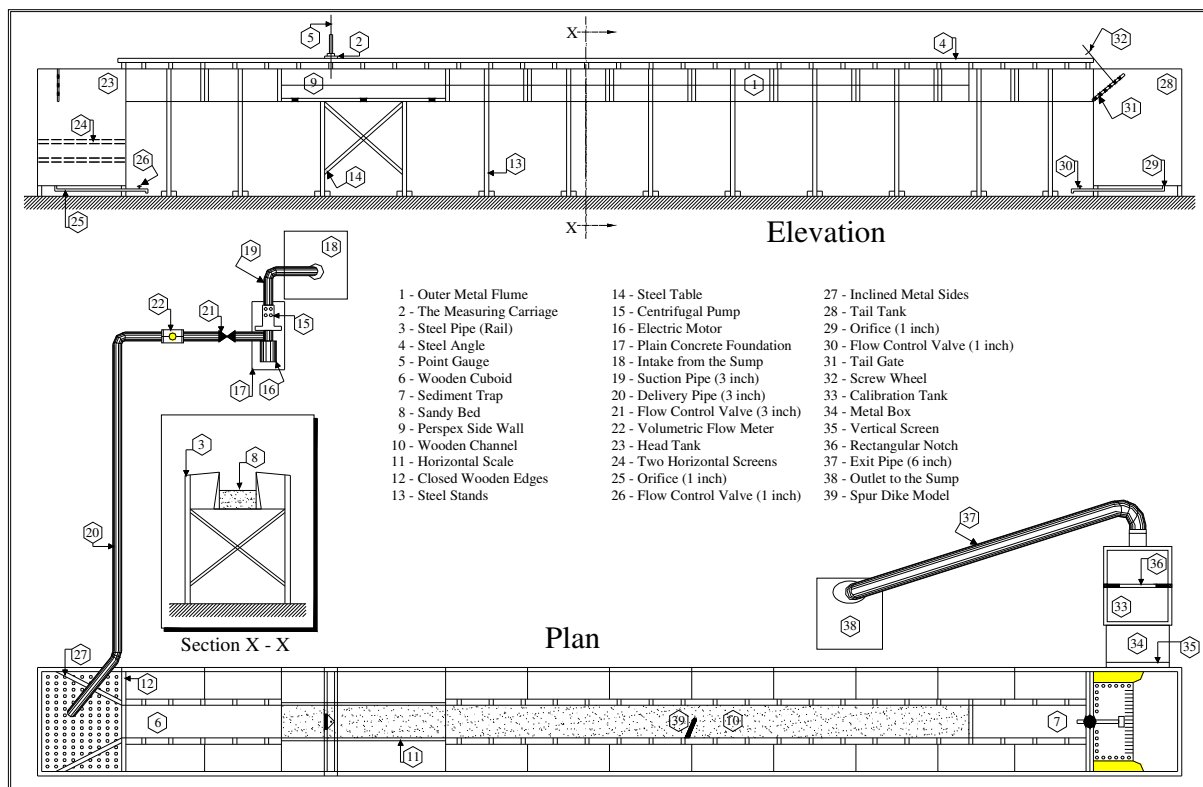
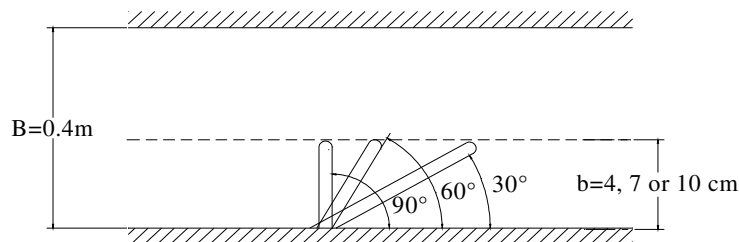


Fig.(1). Scheme of experimental apparatus and circulating system.

## EXPERIMENTAL SETUP

The experimental program was performed at the Irrigation and Hydraulic Laboratory, Faculty of Engineering, Mansoura University. A re-circulating flume of 12m long, 0.4m wide and 0.4m deep was used. A horizontal scale with accuracy of 1.0mm was fixed along the flume for measuring the horizontal distances. A point gauge with a harp edged end and with a venire scale, was installed on a manually carriage running along the flume to measure the bed elevation, the water depth and the scour hole geometry. Medium sand was used as bed material with depth equals to 0.20m. The flume is provided with centrifugal pump to recirculate the water from ground tank to feed the flume with the required flow discharge. Figure (1) shows the layout of the flume.

To achieve the research objectives, nine spur-dike models were made in three different groups. The first group was aligned perpendicular to the flow, the second and the third groups were aligned with an angle  $60^\circ$  and  $30^\circ$  respectively. For each group, there were three models with three different lengths to achieve the proposed contraction ratios, Fig. (2).



**Fig. (2) Spur dike models**

## DIMENSIONAL ANALYSIS

Dimensional analysis was applied to develop the relationship between the maximum scour hole depth and length with the other variables involved in the phenomena. In this study, the maximum scour depth,  $d_s$ , is the dependent variable and can be expressed as a function of other independent variables as follows.

$$d_s = f(g, \nu, \rho, H, V, V_c, B, b, \theta, S, L_{up}, L_{down}) \quad (1)$$

Where:  $g$  = gravitational acceleration,  $\rho$  = fluid density,  $\nu$  = fluid kinematics viscosity,  $H$  = depth of approach flow upstream of the piles,  $V$  = mean flow velocity,  $V_c$  = critical flow velocity,  $B$  = channel width,  $b$  = length of obstruction,  $\theta$  = angle of attack,  $S$  = shape factor,  $L_{up}$  = Length of scour upstream the spur dike,  $L_{down}$  = Length of scour downstream the spur dike.

The equation could be rearranged to:

$$d_s/H = K_\theta K_s \varphi ( F_r, V/V_c, e, L_{up}/H, L_{down}/H) \quad (2)$$

where:

$K_\theta$ ,  $K_s$  = alignment and shape factors respectively,  $F_r$  = Froude number and  $E$  = contraction ratio =  $b/B$ .

## TEST PROCEDURE

The following procedure was followed to conduct each test:

- 1- The spur-dike model was placed in the study reach and fixed well to prevent any movement.
- 2- The bed material was leveled to insure that all points of the bed had the same elevation.
- 3- A tail gate was kept temporarily closed until the flume was filled up in a very low flow rate to avoid any disturbance for the bed elevation.
- 4- The required discharge was allowed to flow gradually until it reaches a constant value.
- 5- The tail gate was lowered gradually until it reaches the required water depth, then start time of run is recorded.
- 6- As soon as the run time was over, the flow discharge has been stopped then the water was drained slowly in order to prevent sediment movement. After the channel was dried, the measurements can be conducted.

## EXPERIMENTAL RESULTS

From Figures (3) to (6), which show the contour map of scour holes, it can be concluded that the hole geometry has the following characteristics:

- The scour hole side slop is steep at upstream of the spur, but the downstream portion of the hole is elongated in the downstream direction and has a milder slope. The difference in side slopes is due to the higher flow energy and turbulence in the upstream than the downstream.
- The scour hole has the approximate form of an inverted frustum cone with its vertex representing the point of maximum depth which is almost occurs near the groin tip.
- In most cases, the base of the scour hole with spur dikes having orientation angles of  $90^\circ$  and  $60^\circ$  is nearly rectangular and oriented at the upstream face of the spur. But with those having an orientation angle of  $30^\circ$ , the base of scour hole is circular with its center on the extent of the spur longitudinal centerline.

In addition, longitudinal sections through the scour hole at the groin tip were taken to figure out the scour hole lengths and side slopes upstream and downstream the structure. Figures (8) up to (10) show these longitudinal sections. Also, Table (1) gives exact values of the surface of the scour holes extents. Figure (11) shows a definition sketch for the measured ratios in this table. From these figures and from Table (1), the following conclusions can be drawn:

- The upstream side slope is nearly equal to the wet angle of repose of the sediment bed, while the downstream average slope is about 50% of the value. These side slopes angles for the non-uniform sand used in the present study, were about  $33^\circ$  at the upstream and the transverse side is about  $15^\circ$ .
- The upstream length of the scour hole has an average value of  $2b$ . And the downstream portion extents for about  $3b$  to  $4b$ .
- All the transverse sections passing by the groin tip have identical lengths and side slopes to the corresponding upstream sections.
- The upstream length of the scour hole is nearly twice the scour hole depth ( $d_s$ ), and the downstream scour length has an average value of  $4d_s$ .

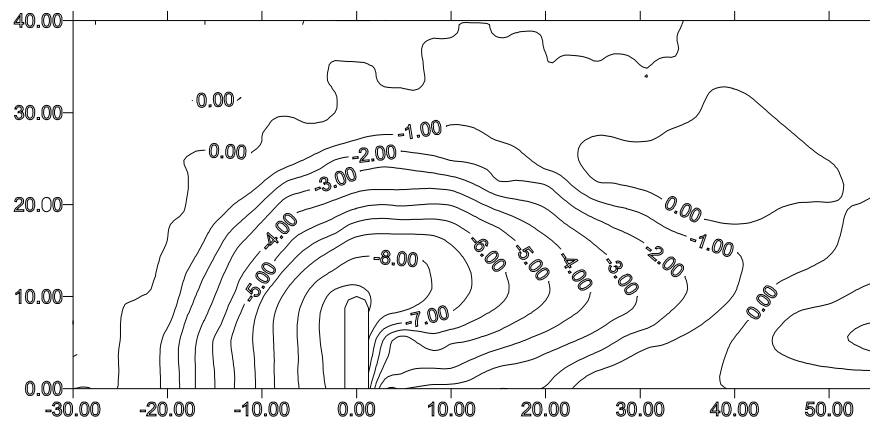


**Fig. (3) Scour hole contour map [  $\theta=90^\circ$ ,  $e=25\%$ ,  $F_r=.29$  ]**

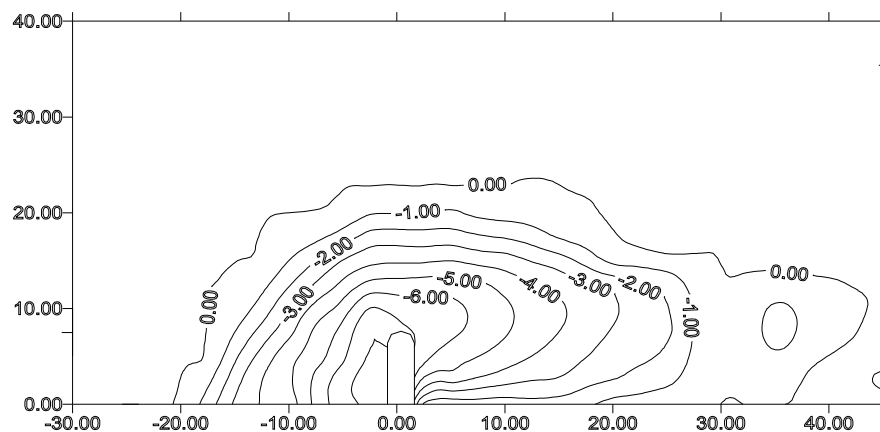


**Fig. (4) Scour hole contour map [  $\theta=90^\circ$ ,  $e=17.5\%$ ,  $F_r=.36$  ]**

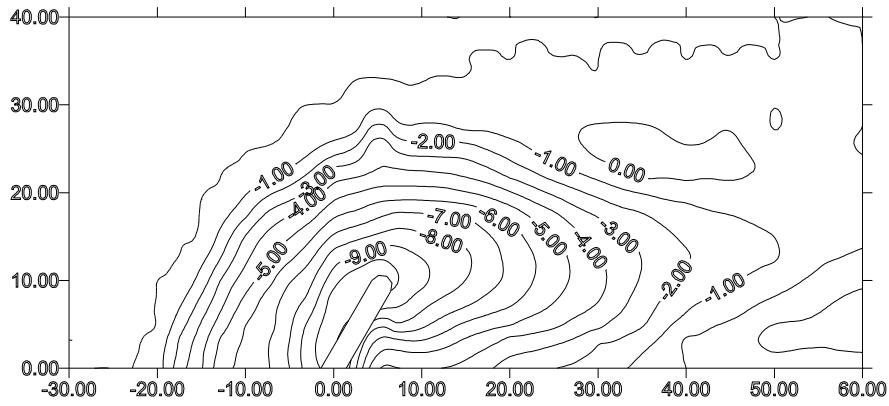


**Fig. (5) Scour hole contour map [ $\theta=60^\circ$ ,  $e=25\%$ ,  $F_r=.35$  ]**

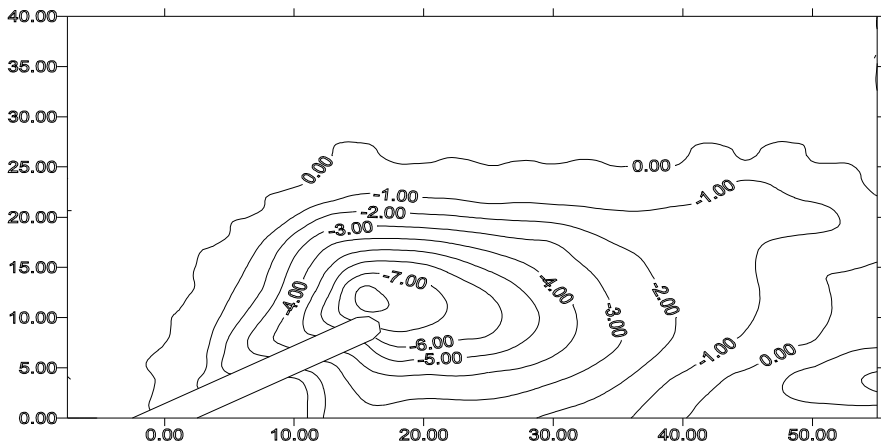


**Fig. (6) Scour hole contour map [ $\theta=30^\circ$ ,  $e=25\%$ ,  $F_r=.35$  ]**

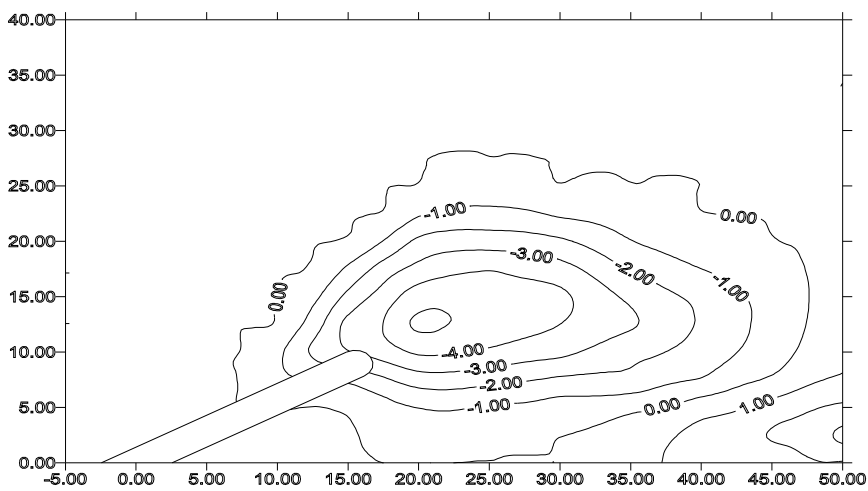


**Fig. (7) Scour hole contour map [ $\theta=30^\circ$ ,  $e=25\%$ ,  $F_r=.29$  ]**

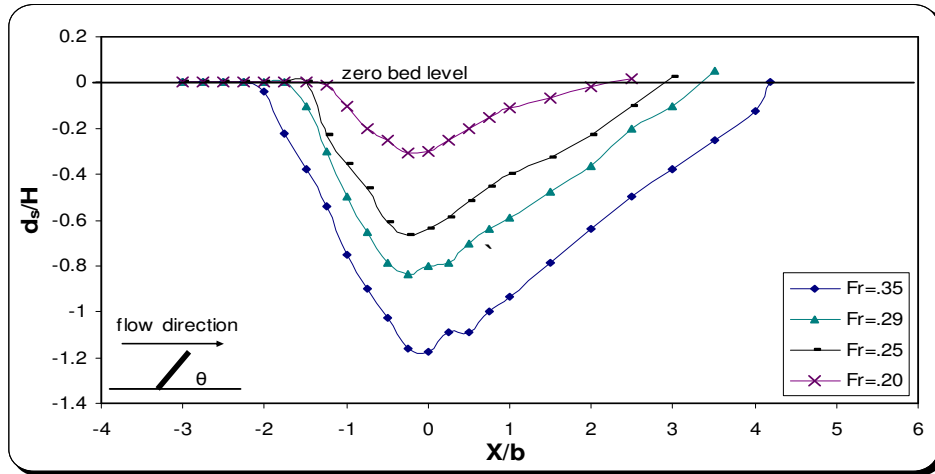


Fig. (8) Longitudinal sections at the spur-dike tip corresponding to different Froude no. [ $\theta=90^\circ$ ,  $e=25\%$ ]

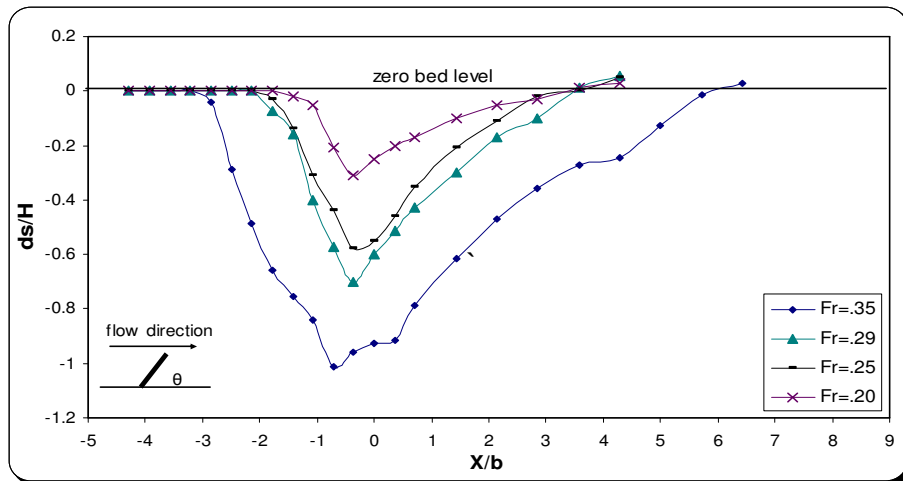


Fig. (9) Longitudinal sections at the spur-dike tip corresponding to different Froude no. [ $\theta=60^\circ$ ,  $e=17.5\%$ ]

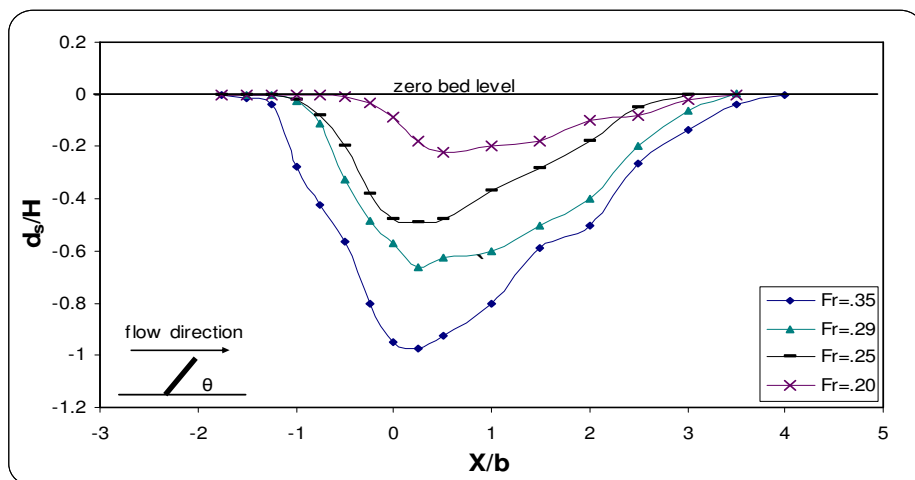
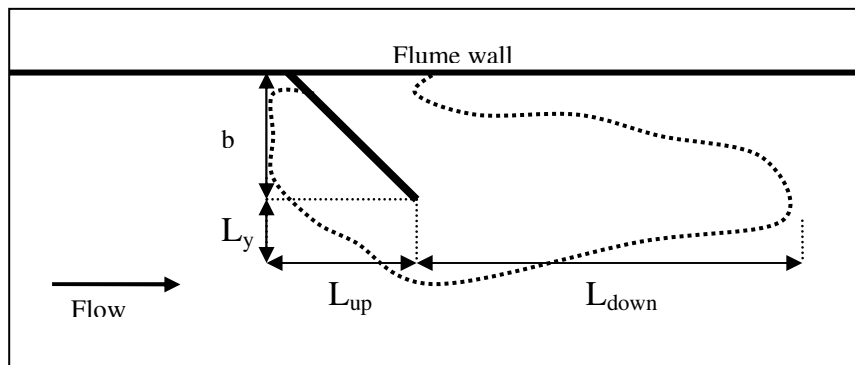


Fig. (10) Longitudinal sections at the spur-dike tip corresponding to different Froude no. [ $\theta=30^\circ$ ,  $e=25\%$ ]

**Table (1) Slope and normalized depth and length of the scour hole**

$\theta$	e %	$F_r$	$d_s/b$	$L_{up}/b$	$L_{down}/b$	$L_y/b$	$\theta_{up}$	$\theta_y$	$\theta_{down}$
90°	25	0.35	0.97	2.3	4.4	2.1	31	32	13.5
		0.25	0.81	1.8	2.8	1.6	29	30	15
		0.19	0.35	1.0	2.4	1.2	32	29	15
		0.29	0.73	1.6	3.0	1.6	30	29	16
		0.2	0.33	1.1	2.1	1.0	33	22	9
	17.5	0.35	1.21	2.6	5.4	2.3	33	30	9
		0.25	0.64	1.5	3.5	1.6	33	30	7
		0.19	0.26	0.9	3.1	0.9	27	18	12
		0.28	0.77	2.1	3.2	1.7	32	31	11
		0.2	0.33	1.5	2.2	1.0	28	23	23
	10	0.36	1.15	3.7	4.6	2.6	28	22	16
		0.25	0.90	2.5	2.0	1.5	33	31	26
		0.28	0.98	2.5	2.0	2.0	33	24	30
		0.2	0.28	1.5	1.0	1.1	24	24	12
	60°	25	0.35	1.09	2.5	5.2	2.3	33	31
0.25			0.75	2.0	2.8	1.6	30	30	16
0.19			0.48	1.1	2.4	1.1	33	32	10
0.28			0.77	2.0	3.5	1.7	33	34	10
17.5		0.35	1.01	2.7	6.8	2.7	35	29	12
		0.25	0.83	1.7	3.1	1.8	34	30	14
		0.28	0.70	1.6	3.4	1.8	31	31	15
10		0.35	1.01	2.0	4.0	2.5	34	32	13
		0.28	0.68	2.075	2.8	2	28	26	11
		0.25	0.63	2	3.3	2.1	34	25	11
30°	25	0.36	0.78	1.7	4.0	1.7	35	37	20
		0.25	0.51	1.3	2.5	1.4	34	29	21
		0.19	0.26	0.7	2.7	1.6	27	24	12
		0.29	0.53	1.0	2.9	1.2	33	31	22
	17.5	0.35	0.96	2.7	4.8	2.0	34	37	20
		0.25	0.56	1.5	3.3	1.7	34	29	21
		0.28	0.67	1.5	2.8	2.0	33	31	12
	10	0.35	0.85	2.5	3.3	2.5	32	24	17
		0.25	0.33	0.8	4.0	1.9	11	11	11
		0.28	0.35	1.5	5.0	1.8	15	17	10



**Fig. (11) Definition sketch for ratios in Table (1)**



## **ANALYSIS AND DISCUSSION**

### **Effect of Flow Conditions on Scour Hole Characteristics**

Due to groin installation, the flow width decreases in some places which in turn changes the velocity profile in the region around the contracted width. Hence, the flow velocity and Froude number are considered very important measures of the flow condition which play a main role in analyzing the scour hole characteristics around a spur-dike. Increasing stream velocity and Froude means increasing the carrying capacity of water and its capability to create scour holes. For these reasons different flow conditions, namely with  $F_r = 0.10, 0.15, 0.2, 0.25, 0.29, 0.35$ , were applied to each model, to investigate the influence of flow condition on scour hole depth and width. As a consequence of increasing the value of Froude number, the ratio  $V/V_c$  increases, in such a manner that the maximum value of this ratio was not exceed the unity, because all experiments were held under clear water conditions as stated before.

From Figures (12) to (15), it is obvious that for different contraction ratios and angels of orientation, all of the scour parameters increased as Froude number increased. On the other hand, the rate of increase of relative scour depth and length decreases as the contraction ratio decreases, because with small contraction ratio the effect of spur dike on flow velocity get smaller. The best fit between Froude number and relative scour parameters in all cases was found to be linear. Also, from Table 2, it can be concluded that for  $F_r = 0.35$  the maximum scour depth is nearly equal to  $1.0b$  for all models. But for  $F_r$  ranging between 0.25 and 0.30 the maximum scour depth has an average value of  $0.8b$  for all models expect those with an orientation of  $30^\circ$ , this value is reduced to  $0.5b$ . As  $F_r$  gets smaller, this value gets smaller until it approaches zero with  $Fr \leq 0.15$  for all models. Furthermore, changing the value of Froude number has no effect neither on the general layout of the scour hole nor its side slopes. Just the case with  $Fr \leq 0.20$  and  $\theta = 30^\circ$  can be expected, as the side slopes get milder. Thus, neglecting the effects of flow conditions for short spur dikes or abutments, as done by some researchers as Melville (1992) and Rahman et al. (2004), is relatively inaccurate. On contrary, it must be emphasized on its essential effects.

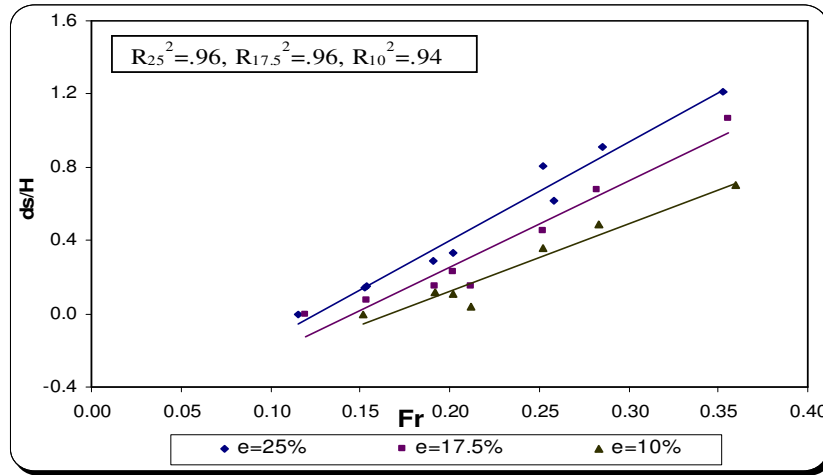


**Fig. (12) Scour hole relative depth as a function of Froude number ( $\theta=90^\circ$ )**

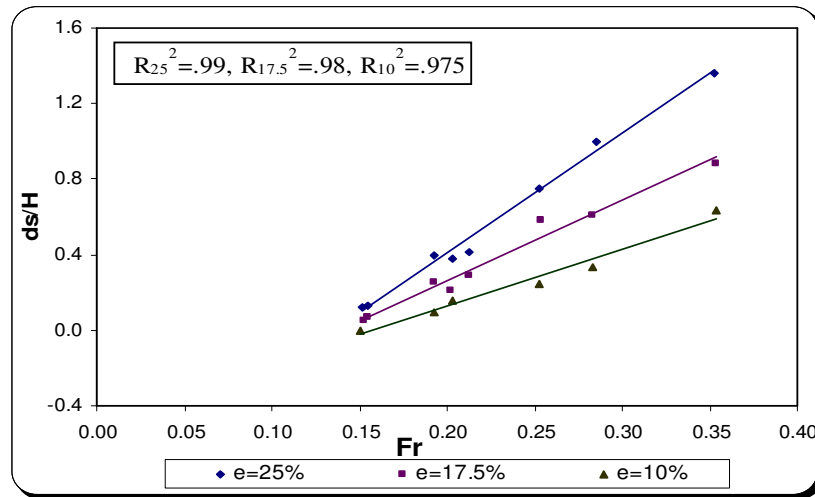


**Fig. (13) Scour hole relative depth as a function of Froude number ( $\theta=60^\circ$ )**

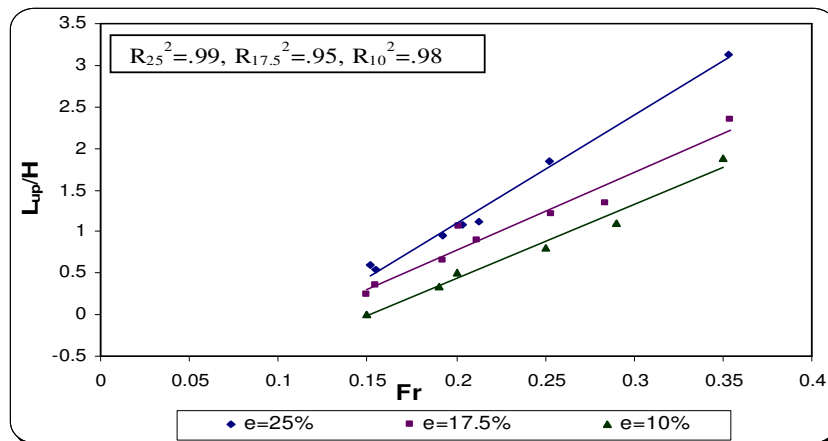


**Fig. (14) Scour hole relative upstream length as a function of Froude number ( $\theta=60^\circ$ )**

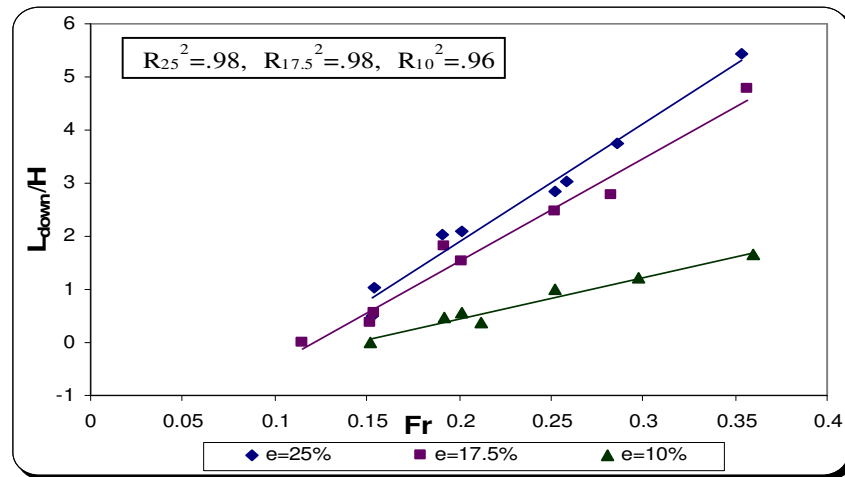
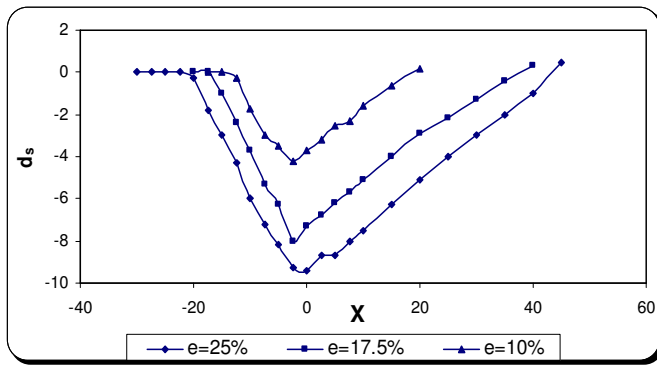


Fig. (15) Scour hole relative downstream length as a function of Froude number ( $\theta=90^\circ$ )

### Effect of Contraction Ratio on Scour Hole Characteristics

By changing the contraction ratios, this leads to a great change in a scour depth and length. In this study the effects of the contraction ratio on the scour hole depth and length are investigated for both the different flow conditions and angles of inclination, using three different contraction ratio, namely 25%, 17.5% and 10%. Figure (16) and Figure (17) show a comparison between scour hole longitudinal sections for different contraction ratios under constant flow conditions and orientations. From these figures, it is obvious that the scour hole depth and length increase as the contraction ratio increases, and this is the same trend with the previous studies. Increasing the contraction ratio, i.e. decreasing the width available to water to pass by, results in inducing more flow patterns disturbance and higher velocities which in turn increases the down flow, horseshoe vortex that considered the main cause of scouring process, and increases other vortices strength with the increase of obstruction length.

Also, it can be concluded that the contraction ratio effect disappeared gradually with smaller Froude number, even for higher values of  $e$ , because at this case the vortex power get so weak to produce pronounced distribution on the original bed, and its effect is limited to deflect the flow patterns. In addition, increasing the contraction ratio than 25% with higher values of Froude number, will danger the stability of the opposite bank, in addition to the stability of the spur it self, which will cost a lot to protect the spur foundation and the channel banks against the scouring process.



**Fig. (16) Scour hole longitudinal sections for different contraction ratios ( $\theta=90^\circ$ ,  $Fr=.35$ )**

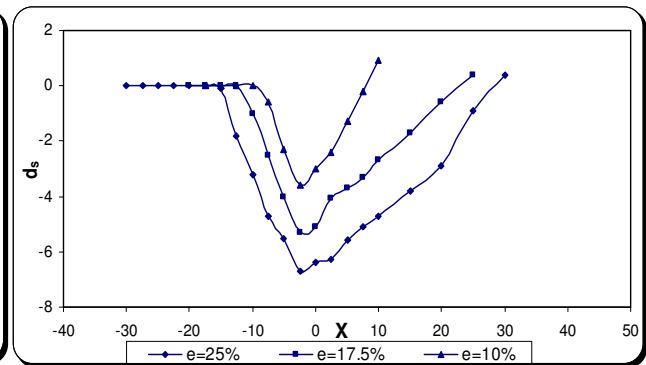


**Fig. (17) Scour hole longitudinal sections for different contraction ratios ( $\theta=90^\circ$ ,  $Fr=.29$ )**

### Effect of Spur Dike Alignment

Spur dikes may be positioned facing upstream (repelling groin), normal to flow (deflecting groin), or facing downstream (attracting groin). Each orientation to the flow affects the river current in a different way. The present study is limited on the cases of deflecting and attracting groins. The angle tested in this study was  $90^\circ$ ,  $60^\circ$  and  $30^\circ$ . Figures (18) to (20) show the effect of the three angle of orientation used in this study. It can be postulated from these figures, that for all contraction ratios and flow conditions, the angle  $30^\circ$  has an obvious effect on reducing the scour depth, because spur-dike with angle  $30^\circ$  dose not act as an obstacle for flow as that with angle  $60^\circ$  or  $90^\circ$ , in another word it's effect on flow velocity is more gentler than greater values of  $\theta$ . Also, from the scour hole contour maps, angle  $30^\circ$  show the best performance in bank protection especially upstream the structure, where the upstream side wall was kept intact even for the high flow conditions, used in this work. For angle  $30^\circ$ , the maximum scour depth occurred just downstream the groin tip, and the base of scour hole is nearly circular.

A number of previous studies indicated that the scour depth is reduced gradually as  $\theta$  changed from  $90^\circ$  to  $30^\circ$ . That is because deflecting groins restricts a greater amount of fluid motion upstream it that the other orientation angles, which in turn increases the flow velocity in the contracted area near the tip. But at general, Spur-dike alignment dose not show a significant effects on scour hole length downstream the spur dike, just for with higher Froude number, angle  $30^\circ$  shows its effect on reducing scour length and angle  $60^\circ$  gives the longer scour hole length in most cases.

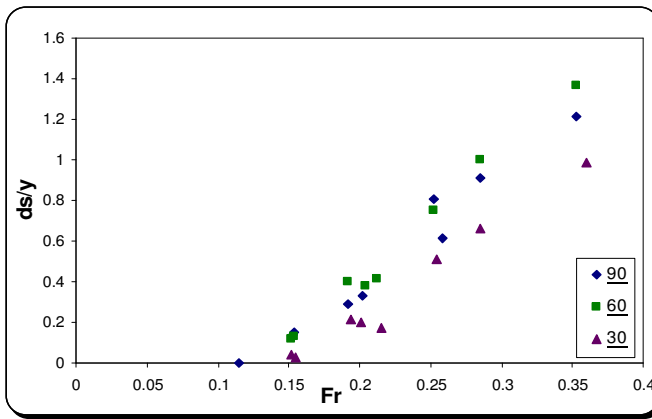


Fig. (18) Variation of scour hole depth with Froude no. (e= 25%)

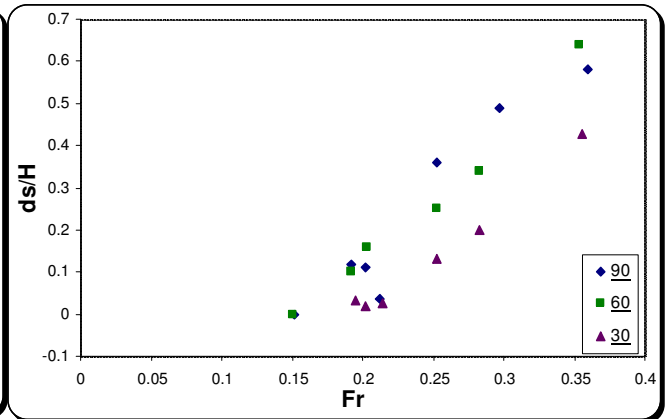


Fig. (19) Variation of scour hole depth with Froude no. (e= 10%)

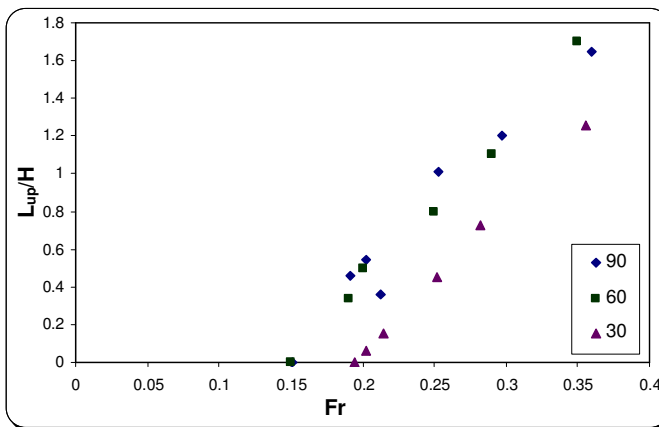


Fig. (20) Variation of scour hole upstream length with Froude no, (e= 10%)

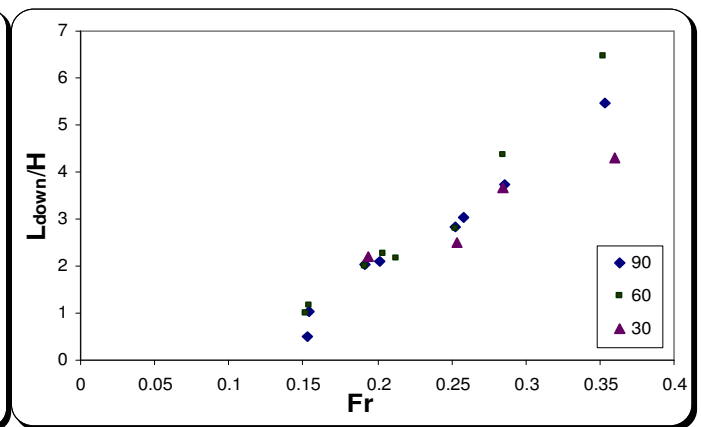


Fig. (21) Variation of scour hole downstream length with Froude no. (e= 25%)

### Development of Equations

Several equations were developed to estimate the scour hole depth and length. All these equations were developed by the regression analysis, using Excel Program.

#### - Proposed Equations for Scour Depth:

$$d_s / H = C_\theta C_e (6.142 F_r - 0.941) \tag{3}$$

where:

$d_s$  = Scour hole depth

H = approach flow velocity  
 F<sub>r</sub> = Froude number  
 C<sub>e</sub>, C<sub>θ</sub> = factors depending on contraction ratio and angle of orientation respectively.  
 Given in Table (2)

**- Proposed Equations for Scour Hole Length Upstream the Structure:**

$$L_{up}/H = C_{\theta} (12.2 * C_e * F_r - 1.4) \tag{4}$$

where

L<sub>up</sub> = scour hole length upstream the spur dike  
 C<sub>e</sub>, C<sub>θ</sub> = factors depending on contraction ratio and spur alignment respectively.  
 Given in Table (2)

**- Proposed Equations for Scour Hole Length Downstream the Structure:**

$$L_{down}/H = C_e ( 21.274 F_r - 2.263 ) \tag{5}$$

Where:

L<sub>down</sub> = scour hole length downstream the spur dike  
 C<sub>e</sub> = a constant depending on contraction ratio. Given in Table (2)

**Table (2) Contraction ratio and alignment factors**

	C <sub>θ</sub>			C <sub>e</sub>			R <sup>2</sup>
	90°	60°	30°	25%	17.50%	10%	
Equation (3)	1.0	0.97	0.83	1.0	0.77	0.5	0.92
Equation (4)	1.0	0.98	0.70	1.0	0.89	0.71	0.91
Equation (5)	-	-	-	1.0	0.85	0.5	0.89

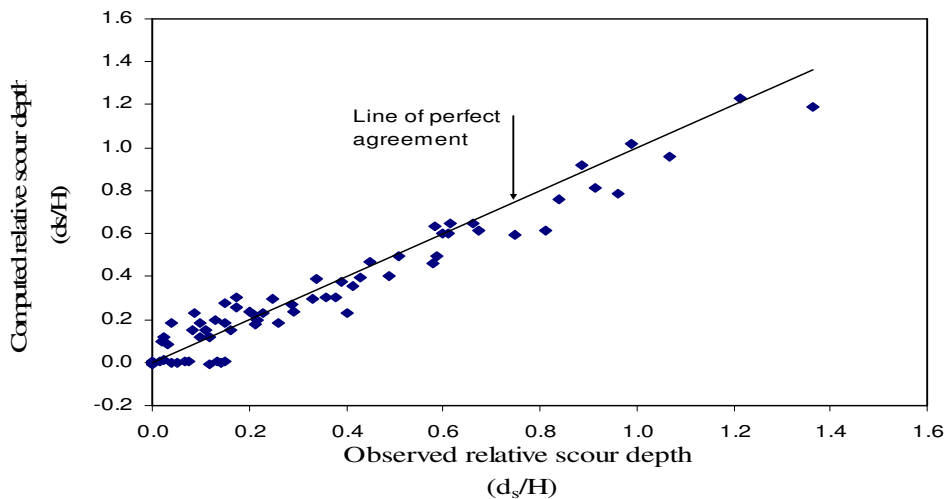


**Fig. (22) The comparison between the computed and observed depth**

**of relative scour depth, Equation (3)**

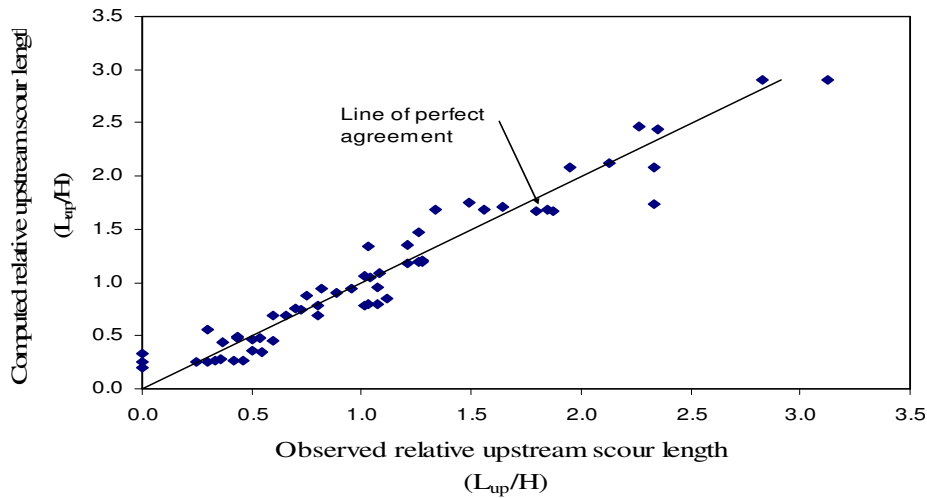


**Fig. (23) The comparison between the computed and observed upstream length of the scour hole, Equation (4)**

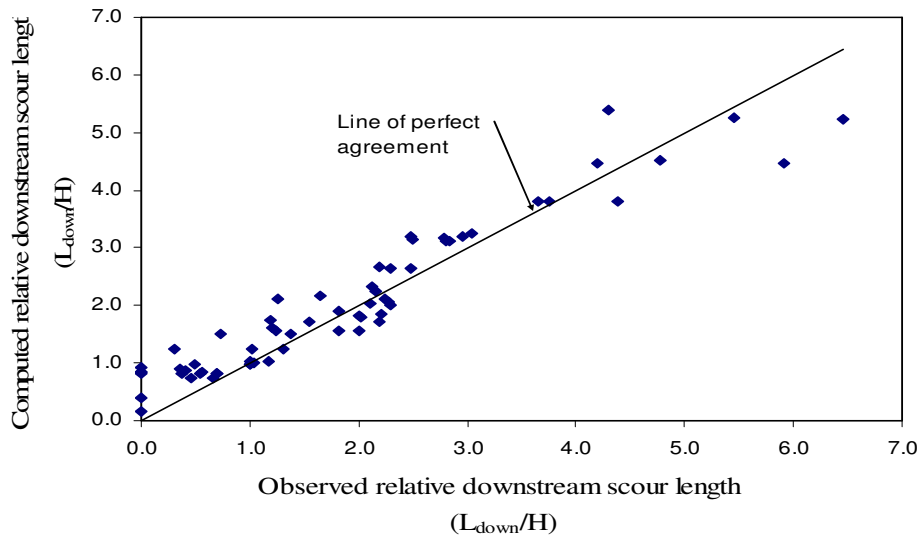


**Fig. (24) The comparison between the computed and observed downstream length of the scour hole, Equation (5)**

**CONCLUSIONS**

A clear water scour experiments were conducted to investigate the characteristics of the scour hole around a single spur-dike installed in a straight flume, the results of these experimental tests were analyzed and discussed and the following conclusions could be drawn from the present study:

- The upstream side slopes are nearly equal to the wet angle of repose of the sediment bed, while the downstream average slope is about 50 to 60% of this angle.
- In most cases, the base of the hole with spur dikes oriented at 90° and 60° is nearly rectangular and oriented at the upstream face of the spur. But with angle 30° the base

of the scour hole is circular with its center located near the groin tip on the extension for its centerline.

- The upstream length of the scour hole has an average value of  $2b$ , and  $4b$  at the downstream side.
- All of the scour parameters increase with the increase of the Froude number with a linear trend. On the other hand, Froude number has no effect on the general layout of the scour hole.
- The relative scour parameters increase with the increase of contraction ratio. But the effect of contraction ratio decreases with small values of Froude number, even for higher values of contraction ratio.
- for the same contraction ratio and flow conditions, angle  $30^\circ$  showed a good performance in reducing the scour depth and in bank protection.
- Angle  $60^\circ$  seems to be unpractical angle for attracting groin. It gave larger and deeper scour hole compared with angle  $30^\circ$ , if other parameters held constant. Also, when compared with angle  $90^\circ$ , it gives an average the same hole dimensions or even larger. In addition, it's actual length will be longer than deflecting groin which leads to higher construction cost.

## SYMBOLS

- B** Channel Width;
- B** Projecting length of Obstruction;
- $C_\theta$**  Alignment Coefficient;
- $C_e$**  Contraction Ratio Coefficient;
- $d_s$**  Maximum Scour Hole Depth;
- E** Contraction Ratio =  $b/B$ ;
- $F_r$**  Froude Number;
- G** Gravitational Acceleration;
- H** Flow Depth;
- V** Mean Velocity of Flow;
- P** Density of Water and
- N** Kinematic Viscosity of Water.

## REFERENCES

1. Bayram, A., and Larson, M.: "Analysis of Scour around a Group of Vertical Piles in the Field", *Journal of Waterway, Port, Coastal, and Ocean Engineering* / July/August 2000, pp. 215-220.
2. Melville, B.W.: "Pier and Abutment Scour: Integrated Approach", *Journal of Hydraulic Engineering*, ASCE, Vol. 123, No. 2, February, 1997, pp. 125-136.



3. Melville, B.W., and Sutherland, A.J.: "Design Method for Local Scour at Bridge Piers", *Journal of Hydraulic Engineering*, ASCE, Vol. 114, No. 10, October, 1988, pp. 1210-1226.
4. Raudkivi, A.J., and Ettema, R.: "Clear Water Scour at Cylindrical Piers", *Journal of Hydraulic Engineering*, ASCE, Vol. 109 No. 3, March, 1983, pp. 338-350.
5. Raudkivi, A.J.: "Functional Trends of Scour at Bridge Piers ", *Journal of Hydraulic Engineering*, ASCE, Vol. 112, No. 1, January, 1986, pp. 1-13.
6. Salim, M. and Jones, J.S.: "Scour Around Exposed Pile Foundations" *Proceedings of the ASCE*, 1999, "North American Water and Environment Congress"; Anaheim, CA.
7. Sheppard, D. M., Odeh, M., and Glasser, T.: "Large Scale Clear-Water Local Pier Scour Experiments" *Journal of hydraulic Engineering*, ASCE (ISSN 0733-9429), Vol. 130, No. 10, October 1, 2004. pp. 957-963.
8. Sumer, B.M., and Fredsøe, J., and Bundgaard, K.: "Global and Local Scour at Pile Groups", *International Journal of Offshore and Polar Engineering*, ASCE (ISSN 1053-5381), Vol. 15, No. 3, September 2005, pp. 204-204.
9. Sumer, B.M., and Fredsøe, J., and Christiansen, N.: "Scour around Vertical Pile in Waves ", *Journal of Waterway, Port, Coastal, and Ocean Engineering*, ASCE, Vol. 118, No. 1, January/February, 1992, pp. 15-31.
10. Sumer, B.M., and Fredsøe, J.: "Wave Scour around Group of Vertical Piles", *Journal of Waterway, Port, Coastal, and Ocean Engineering*, ASCE, Vol. 124, No. 5, September/October, 1998, pp. 248-256.
11. Sumer, M. B., and Fredsoe, J.: "Scour around pile in combined waves and current." *Journal of Hydraulic Engineering*, ASCE, 127(5), 2001, pp. 403-411.
12. Yen, C. L., Lai, J. S., and Chang, W. Y.: "Modeling of 3D Flow and Scouring around Circular Piers", *Proc. Natl. Sci. Counc. ROC(A)* Vol. 25, No. 1, 2001, pp. 17-26.